NEW METHODS FOR RECORDING AND PROCESSING HIGH FREQUENCY MOIRE PATTERNS

by

Helen S. Johnson
University of Alabama in Huntsville
Huntsville, Alabama 35899

James H. Bennewitz
AT&T Bell Laboratories
Murray Hill, New Jersey 07974

T. Dixon Dudderar
AT&T Bell Laboratories
Murray Hill, New Jersey 07974

Donald R. Matthys
Marquette University
Milwaukee, Wisconsin 53233

John A. Gilbert
University of Alabama in Huntsville
Huntsville, Alabama 35899

ABSTRACT

Two techniques for enhancing the potential of high frequency moire interferometry are investigated. A high frequency Ronchi grating is transferred from a suitably processed silicon wafer to a test specimen. Results indicate that the grating can be used to vary sensitivity, and that gratings of nearly any shape and size can be deposited on the surface of a specimen. Further work is suggested to refine the technique. In addition, an automated approach for measuring surface displacement using moire interferometry is described. The method relies on the introduction of a carrier fringe pattern to achieve fringe linearization, and the application of image digitization and computer analysis to determine the magnitude and direction of a specific displacement component.

INTRODUCTION

High frequency moire interferometry is a highly sensitive full-field optical method useful for measurement of surface displacement [1-3]. The technique requires that a reflective high-frequency phase-type grating be transferred from a mold to the surface of the specimen. The mold may be produced optically by exposing a photographic plate to the standing wave interference pattern produced at the intersection of two plane coherent wavefronts. A thin reflective material is deposited on the regularly corrugated surface of the mold and this coating is transferred to the specimen using an epoxy adhesive. When the specimen is appropriately illuminated, the interference of the deposited grating with a reference grating having twice the spatial frequency yields a moire pattern that can be analyzed to measure a selected component of displacement. Since the mold is produced through optical interference, the specimen grating diffracts all usable light energy into the first orders, thereby fixing sensitivity and limiting the range over which displacements can be measured.

Prior research in conventional moire has demonstrated that multiple diffraction orders can be obtained by transferring a Ronchi grating to a test part [4,5]. The molds used in these investigations are of relatively low spatial frequencies (20-40 lines/mm) as compared with those commonly used in high frequency moire (typically 1000-2000 lines/mm), but fringe multiplications of fifty have been reported (using the positive and negative twenty-fifth orders). A portion of the present study explores the use of a suitably processed silicon wafer as a mold for transferring a high frequency Ronchi grating to the specimen surface. The multiple diffraction orders provide a means of varying the sensitivity in areas of high strain gradients.

In other prior related research, interferometric moire patterns are produced by double exposure. In this technique, a carrier fringe pattern associated with a structural component in an "initial" state is superimposed on a modulated carrier pattern associated with the component in a "loaded" state [1-3]. More recent work has shown that interferometric moire patterns can be recorded in real-time using a holographic/fiber optic recording system. In this approach, a holo-camera is used to store information corresponding to the "undeformed" condition of the structural component [6]. The advantage of the real time approach over the earlier double exposure technique is that the investigator is able to continuously measure full-field displacements during the loading process.

A major factor inhibiting full exploitation of the real time moire interferometric technique is the difficulty of getting quantitative results from the interferograms. Indeed, by itself the interferogram does not even contain sufficient information to determine the sign of the displacement component being measured. However, the real difficulty is that in practical cases the interference patterns obtained are frequently so complex that, even if the sign of the displacements were known, a skilled analyst could obtain quantative results only with the expenditure of considerable time and effort. Therefore, if moire interferometry is to be commonly used as a measurement tool, some method of simplifying the analysis of interferograms must be developed. As suggested in reference 6, this simplification can be attained through image processing and computer analysis.

One method for automating the process of analyzing moire interferograms is discussed in the present study. The problem of determining the sign of the displacement, as well as the need to produce a monotonic phase change across the surface under observation, is solved by utilizing the method of carrier fringes. A set of programs has been written so that a camera/computer system can view fringe patterns produced through moire interferometry and, with a knowledge of the phase characteristics of the carrier, measure surface deformation.

INTERFEROMETRIC MOIRE

In high frequency moire interferometry, the surface displacement is related to the moire fringe pattern by the equation

$$U = (1/f)N \qquad (1)$$

where U is the displacement component measured perpendicular to the lines in the reference grating, f is the spatial frequency (the reciprocal of the distance between lines in the reference grating, usually defined as its pitch, p), and N is the order number assigned to fringes in the pattern. The pitch of the reference grating defines the sensitivity of the technique.

In general, the reference grating is created in space by two interfering plane wavefronts (say W and W_1) of coherent light (see Figure 1). The frequency of the interference lines, f, depends on the angle of intersection between the normals to the wavefronts, (shown as 2α), and is characterized by the equation:

$$f = 2\sin(\alpha)/\lambda \qquad (2)$$

where λ is the wavelength of the incident light.

A specimen grating is usually produced by exposing a photographic plate to the zone of interference shown in Figure 1 with sensitivity adjusted to produce interference patterns having twice the pitch of the reference grating. A regularly corrugated mold is produced once the photographic plate is processed. This surface is coated with a thin reflective layer (usually aluminum), and the layer is transferred to the specimen using epoxy.

The corrugated surface of the interferometrically generated mold results from nonuniform shrinkage of the emulsion of the photographic plate during processing. The corrugated profile of the mold is mathematically described by a cosine function, and the transfer to a test part results in a "blazed" specimen grating which displays only the -1 and +1 diffraction orders. These orders are combined using the optical arrangement shown in Figure 2. Sensitivity of the measurement is fixed at half the pitch of the specimen grating.

TRANSFERRING A HIGH FREQUENCY GRATING FROM A SILICON WAFER

Higher diffraction orders could be obtained if it were possible to transfer a Ronchi grating to the specimen. In the past, most Ronchi gratings were mechanically ruled and, therefore, could not be produced with a pitch comparable to that of an interferometrically generated grating. However, improved step and repeat systems (wafer steppers) are now meeting the requirements for submicron design rules in the electronics industry. This

progress has been driven by many factors including improvements in lens design and fabrication, refinements in optical resists, and the ability to retrofit innovations into existing machines. Current projections indicate that optical lithography will eventually be used to produce IC devices with less than 0.5 micron design rules [7-10].

One of the authors (J.H.B.) along with other colleagues working at AT&T Bell Laboratories recently developed a deep ultraviolet step and repeat system capable of achieving 0.5 micron resolution within a 14.5 mm field under routine use, and even higher resolution (0.35 micron) under more limited conditions [7,11]. The major optical components of the stepper are shown in Figure 3. Pulsed laser light, from a KrF excimer laser at 248.4 nm, enters the stepper through the diffusing element which serves to scatter the beam spatially, thereby improving the uniformity of the illumination. The light then enters the scan system which is comprised of a scanning mirror and a lens. The mirror deflects the pulses into the lens at different angles; the lens, in turn, focuses the pulses at different points in the source plane. Beyond the source plane, the light diverges to fill the condenser and is then focused into the projection lens. As a result, the condenser forms an image of the source plane at the entrance pupil of the projection lens. The effect of scanning many pulses is to create an extended source of light which is imaged at the entrance pupil. Spatial coherence can be set by controlling the extent of the scan.

The silicon wafer shown in Figure 4 was manufactured while initially testing this new system. Each small rectangular area contains a regularly structured grating called a meander pattern. The spacing and orientation of these patterns form the basis for evaluating the accuracy of the system. Figure 4 also shows the result of illuminating a portion of the wafer with an unexpanded laser beam. Since the surface profile of the meander pattern closely resembles a square wave, multiple diffraction orders are produced. The diffraction spectrum is comprised of the fundamental frequency corresponding to the pitch of the grating plus higher order harmonics. A specimen grating created using the wafer as a mold also displays a number of diffraction orders when illuminated with laser light. These include the -1 and +1 diffraction orders used in conventional moire interferometry, plus additional orders produced by the higher order harmonics. The main advantages of this approach over the conventional moire interferometric transfer technique are that sensitivity can be varied by working with higher diffraction orders, and that gratings of nearly any shape and size can be generated and transferred to the specimen. For example, variable sensitivity may be desirable when studying deformations on a specimen in regions of high strain gradients, while a circular grating would facilitate measurement of radial displacements.

An effort was made to transfer the surface profile of a meander pattern from a wafer to a specimen made out of PSM-1 (a photoelastic material). A thin layer of epoxy was applied to a the specimen surface and the specimen was placed epoxy side down on to the top of the silicon wafer. Before the epoxy was completely cured, the specimen was pried from the wafer mold. A transparent grating pattern was transferred to the specimen surface and the surface of the silicon wafer remained undamaged. Upon illumination with a coherent source, multiple diffraction orders were observed, and basic feasibility was established.

A second test was conducted to transfer a reflective grating to the specimen in an effort to increase diffraction efficiency and produce higher contrast fringe patterns. An attempt to remove the mold afer the epoxy had cured completely met with limited success, since only a portion of the grating transferred. One of the major problems can be observed in Figure 5 which shows a magnified image of a portion of the specially prepared surface profile of the wafer. The dove-tail profile of the surface not only made it difficult to uniformly coat the wafer with a reflective coating, but prevented the release of the mold once the epoxy had cured. In addition, the meander patterns on the test wafer shown in Figure 4 are not all of the same pitch. Three different spacings were used to test the layout system capabilities of the stepper system. Therefore, when the wafer is used for moire interferometry, displacements are measured at different sensitivities in each rectangular area of the grid transferred to the specimen. Efforts are currently underway to develop larger area, high frequency molds without the undercutting of the original wafer shown in Figure 5. For example, Figure 6 shows the definition of 0.5 micron equal lines and spaces etched into 1.8 microns of HPR-206. In this investigation, the substrate is a device wafer with tantalum silicide and polysilicon over field oxide features, and the surface profile closely resembles a square wave.

DIGITIZATION AND COMPUTER ANALYSIS

Most moire interferometric fringe patterns obtained in practical applications are too complex to be readily amenable to automated analysis. However, a carrier fringe pattern

may be used to achieve fringe linearization. This carrier fringe technique has been previously applied to analyze holo-interferograms [12-16], and involves superimposing a known linear phase shift on the phase changes caused by surface deformation to produce a monotonically changing phase distribution across the interferogram. A similar situation arises in real-time moire interferometry [6]. Fringes of the original interferogram are reduced to "nearly straight" fringes (distortions in the carrier may arise due to preload) on which the deformation is superimposed as a modulation. Such fringes can be read in by a machine vision system. When the fringes in the initial pattern are later subtracted, the original information about the deformation is retrieved. In addition, the known phase characteristics of the initial pattern allow unambiguous determination of the sign of the displacement vector.

The specimen shown in Figure 7 was used to demonstrate the proposed approach. Initial and modulated fringe patterns, shown in Figures 8 and 9, respectively, were obtained using the optical fiber-based moire interferometric recording system shown in Figure 10. Figure 8 contains information due to the carrier and a slight pre-load on the specimen while Figure 9 contains information for the carrier and pre-load plus deformation. In this investigation, an interferometrically generated linear grating was deposited parallel to the Y axis shown on Figure 7 so that in-plane displacements would be measured along the X direction. The carrier pattern was introduced by rotating the specimen in a counterclockwise direction around the Z axis. This rotational mismatch produced a known phase shift between the two wavefronts diffracted from the specimen surface.

The 7 x 7 mm square regions, or windows, superimposed on Figures 8 and 9 (centered at x = 9 mm and y = 6 mm) were individually recorded using a CID camera/digitizer with a resolution of 256 by 256 pixels and a grey scale range of 256 levels. The analysis of column 128 (the vertical center line of the window) was selected to illustrate the technique. Figures 11 and 12 show intensity plots along this column for the initial pattern and the modulated pattern, respectively. Row numbers increase from the bottom to the top of the digitized window.

A computer program was used for analysis. The intensity values from the initial pattern were put through a fast Fourier transform. Working with the spectrum, the program set up a narrow passband centered around the carrier frequency (preload was assumed small when compared to the carrier). All frequencies outside this passband were removed. The program then examined the spectrum of the modulated pattern and removed all high frequencies where signal strength had fallen back to the noise level. The resulting data were then transformed back to the spatial domain using an inverse fast Fourier transform to obtain smoothed intensity distributions. Next the computer located the extrema of the intensity distributions for each filtered fringe pattern. This was done by applying standard methods of data analysis [17] to fit curves through the data points, and then differentiating to locate the desired extrema. Figures 13 and 14 show plots of fringe order versus row number along the vertical centerline of the window associated with the initial and modulated states of the specimen. Fringe order numbers were assigned by starting at the boundary of the window and labeling the first dark fringe as order 0.5. Subsequent fringe orders are assigned increasing values from the bottom to the top of the scan. This scheme assumes clockwise rotation of the specimen. Figure 15 is a plot of relative fringe order number obtained by subtracting fringe orders in the initial pattern from those of the modulated pattern, taking into consideration a sign change caused by counterclockwise rotation of the specimen. The magnitude of the displacement component is found by substituting these relative fringe order numbers into Equation 1.

Absolute displacement values are measured when absolute fringe order numbers are known for both the initial and modulated patterns. Once absolute fringe orders are assigned to the initial pattern, absolute orders can be specified in the modulated pattern from independent knowledge of the displacement of selected points (a fixed boundary, etc.), or by following one of the fringes to its displaced location. Images of the initial and modulated patterns can be stored on video tape. Later, any two images may be chosen, digitized, and numerically subtracted.

In addition to the determination of the sign of the displacement vector, the digital approach outlined above has other advantages. For example, the method requires a simpler set-up than that previously reported for real time analysis; a lower frequency carrier can be used as compared to that required for optical superposition; and, spatial filtering is not required.

The present study demonstrated the feasibility for digitizing and automatically analyzing moire interferograms to measure a single in-plane displacement component. However, a cross grating would facilitate the measurement of the orthogonal in-plane component. In

addition, prior research has demonstrated that out-of-plane displacement information can also be extracted optically from moire interferograms [17]. Optical systems and computer programs are currently being developed to address the task of digitally processing all three displacement components.

RECOMMENDATIONS AND CONCLUSIONS

Some techniques for enhancing the potential of high frequency moire have been investigated. For example, the potential of transferring a high frequency Ronchi grating from a silicon wafer to the surface of a test specimen for moire interferometric analysis has been demonstrated. The main advantages of this approach over the more conventional approach of transferring an interferometrically generated grating are that sensitivity can be varied by working with higher diffraction orders, and that gratings of nearly any shape and size can be generated and transferred to the specimen.

In addition, the use of digital image processing and computer analysis has been shown as an alternative to optical superposition. The major advantage of this approach over the more conventional optical method is that with a knowledge of the initial carrier pattern, the sign as well as the magnitude of the displacement vector is uniquely determined.

Future research will involve combining the new grating and transfer process with computer vision systems to automatically measure three-dimensional displacements, thereby significantly enhancing and extending the moire interferometric technique.

ACKNOWLEDGEMENT

The authors wish to acknowledge support provided by NASA, the Center for Applied Optics at the University of Alabama in Huntsville, Marquette University, AT&T Bell Laboratories; and, the U.S. Army Research Office in Research Triangle Park, N.C. under contract number DAAL 03-86-K-0014. They also wish to express their appreciation to Dan Post and his group at VPI & SU for their guidance and encouragement during the early stages of this research program.

REFERENCES

1. Post, D., "Moire interferometry for deformation and strain studies," Optical Engineering 24(4), 663-667, 1985.

2. Basehore, M.L., Post D., "Displacement fields (u,w) obtained simultaneously by moire interferometry," Applied Optics 21(14), 2558-2562, 1982.

3. Post, D., Czarnek, R., Joh, D., Wood J.D., "Shear strain anomalies in composite beam specimens by moire interferometry," Proceedings of the SEM Spring Conference on Experimental Mechanics, Las Vegas, NV, 916-921, June 1985.

4. Walker, C.A., McKelvie, J., "A practical multiplied-moire system, "Exerimental Mechanics 18(8), 316-320, 1978.

5. Rowlands, R.E., Vallem, J.H., "On replication for moire-fringe multiplication," Experimental Mechanics 20(5), 167-169, 1980.

6. Johnson, H.S., Gilbert, J.A., Matthys, D.M., Dudderar, T.D., "Real time moire interferometry," accepted for publication in Experimental Mechanics.

7. Pol, V., Bennewitz, J.H., Escher, G.C., Feldman, M., Firtion, V.A., Jewell, T.E., Wilcomb, B.E., Clemens, J.T., "Excimer laser-based lithography: a deep ultraviolet wafer stepper," Proc. of SPIE 633, 6-16, March 1986.

8. Miller, V., Stover, H.L., "Submicron optical lithography," Solid State Technology 29, 127, January 1985.

9. Shiotake, N., Yoshida, S., "Recent advances of optical step-and-repeat systems," Proc. of SPIE 537, 168, March 1985.

10. Nakase, M., "The potential of optical lithography," Proc. of SPIE 537, 160, March 1985.

11. Bennewitz, J.H., Escher, G.C., Feldman, M., Firtion, V.A., Jewell, T.E., Pol, V., Wilcomb, B.E., Clemens, J.T., "Excimer laser-based lithography for 0.5 micron device technology," Proc. of the IEEE/IEDM Conference, Los Angeles, California, 312-315, December 1986.

12. Katzir, Y, Friesem, A.A., Glaser, I., Sharon, B., "Holographic nondestructive evaluation with on-line acquisition and processing,"Industrial and Commercial Applications of Holography, Milton Chang, ed, Proc. SPIE 353, 74-82, 1982.

13. Sciammarella, C.A., Ahmadshahi, M., "Computer based method for fringe pattern analysis," Proc. of the 1984 SEM Fall Conference, Milwaukee, WI, 61-69, November 1984.

14. Plotkowski, P.D., Hung, Y.Y., Hovanesian, J.D., Gerhart, G., "Improved carrier technique for unambiguous determination of holographically recorded displacements," Optical Engineering 24, 754-756, 1985.

15. Matthys, D.R., Gilbert, J.A., Dudderar, T.D., "Computer analysis of holo-interferograms," Proc. of the 1986 SEM Spring Conference on Experimental Mechanics, New Orleans, Louisiana, 833-838, June 1986.

16. Matthys, D.R., Dudderar, T.D., Gilbert, J.A., "Automated analysis of holo-interferograms for determination of surface displacements," accepted for publication by Experimental Mechanics, 1987.

17. Basehore, M.L., Post, D., "Moire method for in-plane and out-of-plane displacement measurements," Experimental Mechanics 21(9), 321-328, 1981.

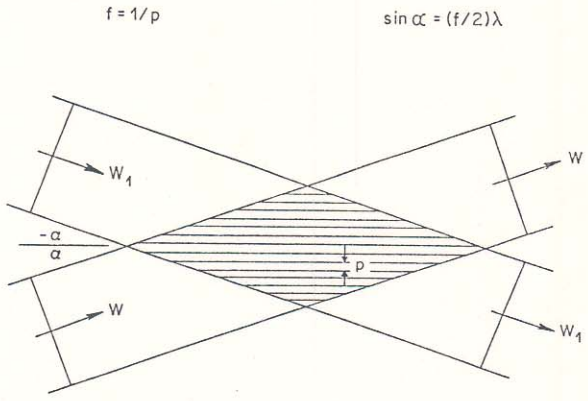

Figure 1. Interference Zone of Two Plane Wavefronts of Coherent Light.

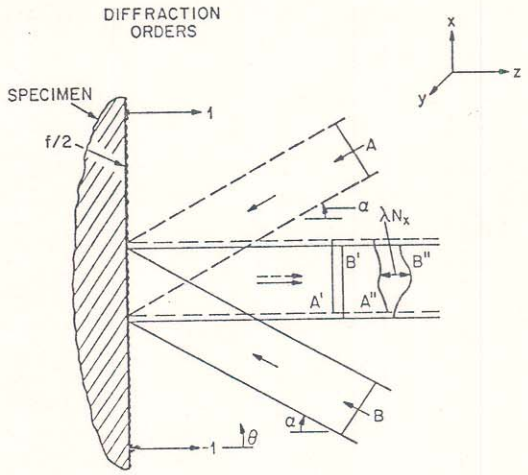

Figure 2. First Order Wavefront Diffraction in Moire Interferometry.

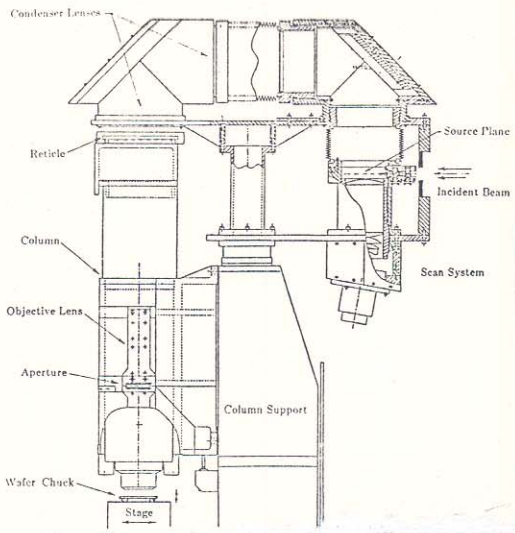

Figure 3. Stepper Illumination and Projection Optics (Side View).

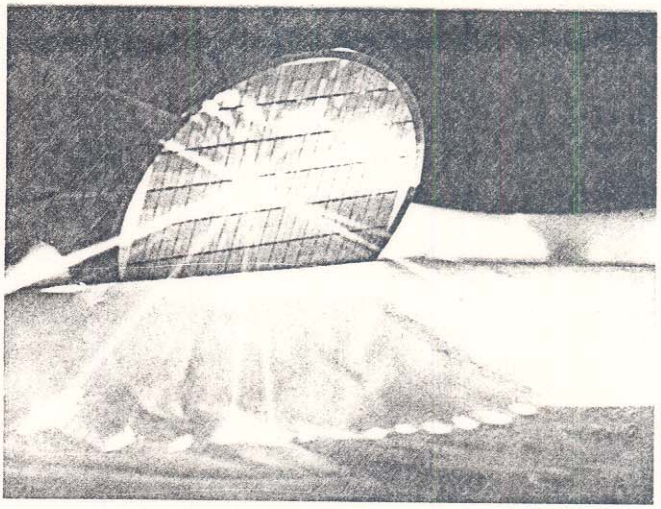

Figure 4. Laser Illuminated Silicon Wafer with Meander Pattern.

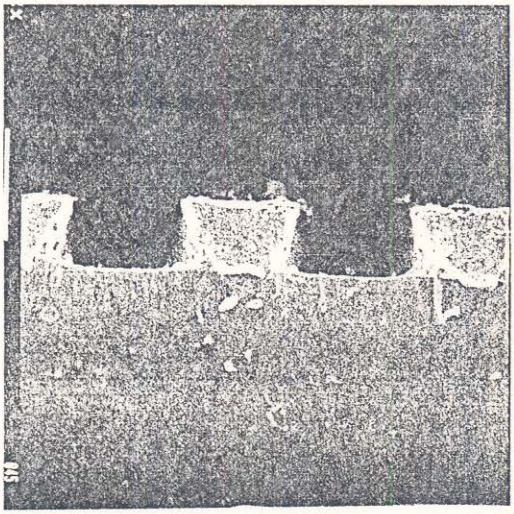

Figure 5. Surface Profile of a Meander Pattern.

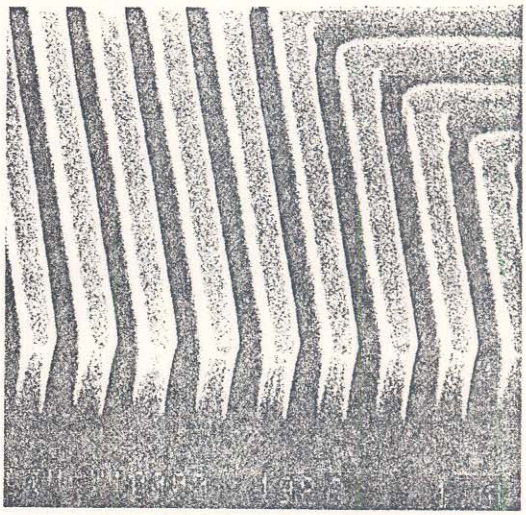

Figure 6. A 0.5 Micron Resolution Test Pattern.

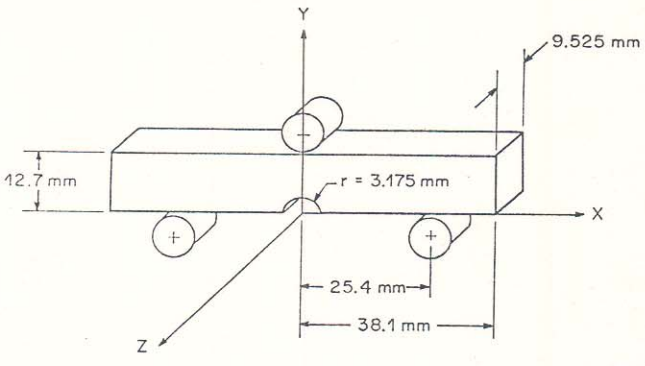

Figure 7. Notched Beam Specimen.

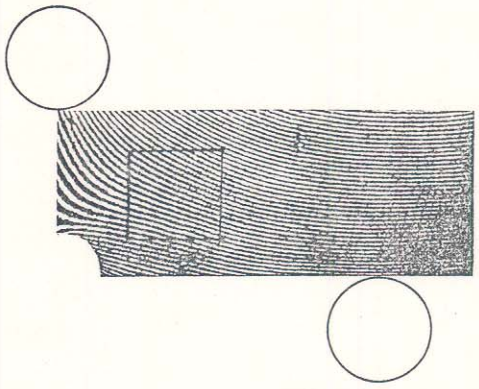

Figure 8. Initial High Frequency Moire Pattern with Digitized Window.

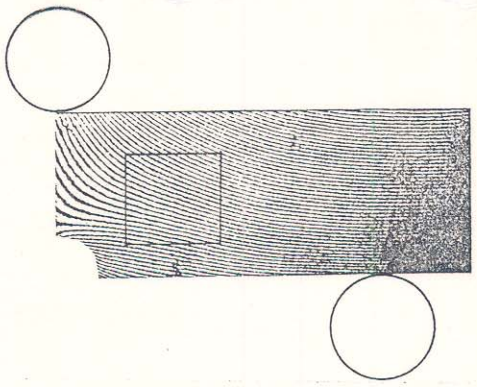

Figure 9. Modulated High Frequency Moire Pattern with Digitized Window.

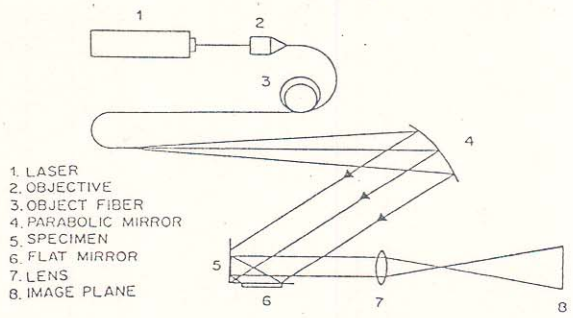

Figure 10. Fiber-Based Moire Interferometric Recording System.

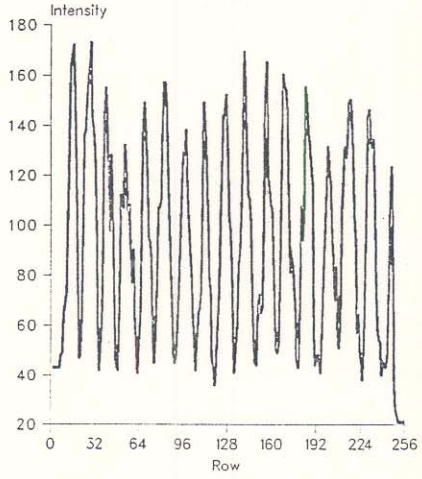

Figure 11. Intensity Plot along Vertical Center Line of the Window Shown in Figure 8.

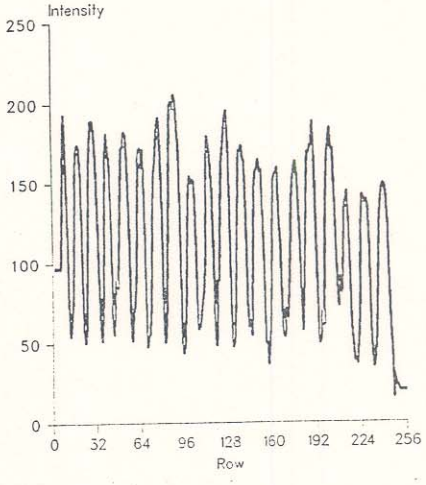

Figure 12. Intensity Plot along Vertical Center Line of the Window Shown in Figure 9.

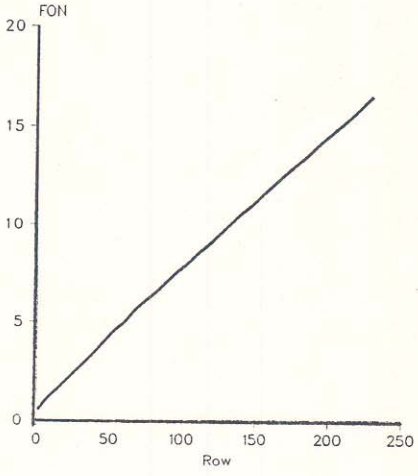

Figure 13. Fringe Data along the Vertical Center Line of the Window Shown in Figure 8.

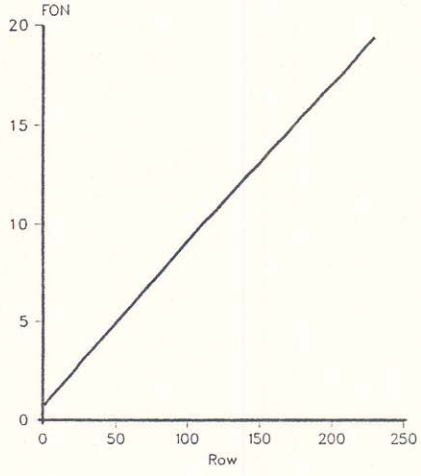

Figure 14. Fringe Data along the Vertical Center Line of the Window Shown in Figure 9.

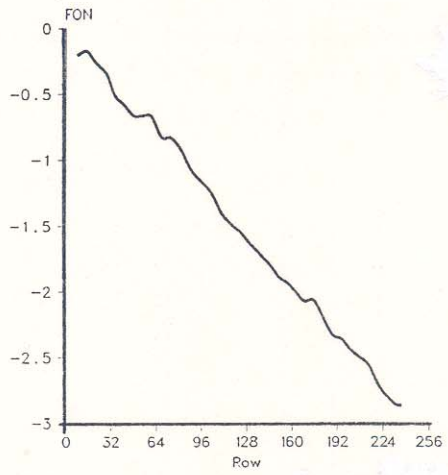

Figure 15. Relative Fringe Orders along the Vertical Center Line of the Window.